



**HAL**  
open science

# Analysis of size effects in $\text{Pb}(\text{Zr}_{0.54}\text{Ti}_{0.46})\text{O}_3$ thin film capacitors with platinum and $\text{LaNiO}_3$ conducting oxide electrodes

R. Bouregba, N. Sama, Caroline Soyer, Denis Remiens

► **To cite this version:**

R. Bouregba, N. Sama, Caroline Soyer, Denis Remiens. Analysis of size effects in  $\text{Pb}(\text{Zr}_{0.54}\text{Ti}_{0.46})\text{O}_3$  thin film capacitors with platinum and  $\text{LaNiO}_3$  conducting oxide electrodes. *Journal of Applied Physics*, 2009, 106 (4), pp.044101. 10.1063/1.3200956 . hal-00473708

**HAL Id: hal-00473708**

**<https://hal.science/hal-00473708>**

Submitted on 25 May 2022

**HAL** is a multi-disciplinary open access archive for the deposit and dissemination of scientific research documents, whether they are published or not. The documents may come from teaching and research institutions in France or abroad, or from public or private research centers.

L'archive ouverte pluridisciplinaire **HAL**, est destinée au dépôt et à la diffusion de documents scientifiques de niveau recherche, publiés ou non, émanant des établissements d'enseignement et de recherche français ou étrangers, des laboratoires publics ou privés.

# Analysis of size effects in $\text{Pb}(\text{Zr}_{0.54}\text{Ti}_{0.46})\text{O}_3$ thin film capacitors with platinum and $\text{LaNiO}_3$ conducting oxide electrodes

Cite as: J. Appl. Phys. **106**, 044101 (2009); <https://doi.org/10.1063/1.3200956>

Submitted: 03 September 2008 • Accepted: 11 July 2009 • Published Online: 19 August 2009

R. Bouregba, N. Sama, C. Soyer, et al.



View Online



Export Citation

## ARTICLES YOU MAY BE INTERESTED IN

[Investigation of thickness dependence of the ferroelectric properties of  \$\text{Pb}\(\text{Zr}\_{0.6}\text{Ti}\_{0.4}\)\text{O}\_3\$  thin-film capacitors](#)

Journal of Applied Physics **99**, 034102 (2006); <https://doi.org/10.1063/1.2170414>

[Interface-induced phenomena in polarization response of ferroelectric thin films](#)

Journal of Applied Physics **100**, 051607 (2006); <https://doi.org/10.1063/1.2337009>

[Interface depolarization field as common denominator of fatigue and size effect in  \$\text{Pb}\(\text{Zr}\_{0.54}\text{Ti}\_{0.46}\)\text{O}\_3\$  ferroelectric thin film capacitors](#)

Journal of Applied Physics **107**, 104102 (2010); <https://doi.org/10.1063/1.3380837>

Lock-in Amplifiers  
up to 600 MHz



Zurich  
Instruments



# Analysis of size effects in $\text{Pb}(\text{Zr}_{0.54}\text{Ti}_{0.46})\text{O}_3$ thin film capacitors with platinum and $\text{LaNiO}_3$ conducting oxide electrodes

R. Bouregba,<sup>1,a)</sup> N. Sama,<sup>2</sup> C. Soyer,<sup>2</sup> and D. Remiens<sup>2</sup>

<sup>1</sup>Laboratoire CRISMAT-ENSICAEN, Université de Caen, CNRS UMR 6508, Boulevard du Maréchal Juin, 14050 Caen Cedex, France

<sup>2</sup>IEMN-DOAE, CNRS UMR 8520, Cite Scientifique, 59655 Villeneuve D'Ascq Cedex, France

(Received 3 September 2008; accepted 11 July 2009; published online 19 August 2009)

The problem of thickness dependence of dielectric and ferroelectric properties of  $\text{Pb}(\text{Zr}_{0.54}\text{Ti}_{0.46})\text{O}_3$  (PZT) thin film capacitors is addressed. Experimental data collected on PZT capacitors with different thicknesses and different electrode configurations, using platinum and  $\text{LaNiO}_3$  conducting oxide, are examined within the prism of existing models. Available literature data, abounding but contradictory, led us to conclude that in the range of thickness investigated, size effect under all its aspects, i.e., increase in coercive field ( $E_c$ ) as well as decrease in both dielectric permittivity and remnant polarization ( $P_r$ ), result basically from existence of a depolarization field. It is shown however that the latter arises from interface chemistry, mostly related to the upper surface of the films, instead of finite screening length in the electrodes unlike commonly accepted. Moreover it is established that increase in  $E_c$  and decrease in  $P_r$  are not concomitant, and significant degradation of one or the other of these values strongly depends on whether a static potential, due to charged defects, is present or not at this interface. © 2009 American Institute of Physics.

[DOI: [10.1063/1.3200956](https://doi.org/10.1063/1.3200956)]

## I. INTRODUCTION

The continual increase in memory density demands permanent effort of devices miniaturization. This is the case of ferroelectric random access memories (FRAMs), the pursuit of scalability of which requires switching voltage increasingly low in order to minimize power consumption. Unfortunately, reduction in the thickness of ferroelectric thin films used in FRAM comes with an increase in the electric field necessary for reversing the polarization (the coercive field  $E_c$ ), what considerably hinders downscaling of the switching voltage. For 20 years,  $\text{Pb}(\text{Zr}_x\text{Ti}_{1-x})\text{O}_3$  (PZT) perovskite has been one of the most investigated ferroelectric material for FRAM applications.<sup>1</sup> However degradation of the properties of ferroelectric films with reduced thicknesses is a general issue that concerns various materials and for the past 50 years, this problem has been the subject of a considerable number of experimental and theoretical works. An increase in  $E_c$  (Refs. 2–9) and a decrease in both dielectric permittivity ( $\epsilon_r$ ) (Refs. 4, 10, and 11) and remnant polarization ( $P_r$ ) were indeed often reported, although this last point has been experimentally underlined since only recently on epitaxial PZT and  $\text{BaTiO}_3$  (BTO) ferroelectric capacitors with oxide conducting electrodes.<sup>12–14</sup> Many mechanisms have been invoked and models developed, to describe size effects in ferroelectric films: homogeneous surface nucleation of domains of opposite polarity [Janovec–Kay–Dunn (JKD) theory],<sup>3,15</sup> depolarization field resulting from incomplete compensation of bound polarization charges by free charges in the electrodes,<sup>16–18</sup> presence of “dead” layer with low dielectric constant at ferroelectric/electrode interfaces,<sup>2,4,5,10</sup> grain size dependence of domain structure,<sup>7</sup> and more re-

cently first-principles calculations on BTO capacitor including realistic ferroelectric-electrode interfaces.<sup>19</sup> The latter work was carried out within the framework of the growing interest drawn to the fundamental problem of disappearance of ferroelectricity in ultrathin perovskite films. Moreover, some of the works mentioned above call for mechanisms different from each other according to the investigated parameter, such as interface passive or dead layer for degradation of  $\epsilon_r$ , depolarization field due to finite screening length in the electrodes for loss of polarization, and surface nucleation for degradation of  $E_c$ , knowing moreover that interface passive layers have been demonstrated not be relevant to explain the degradation of  $E_c$ , unless interface charge is considered.<sup>20–22</sup> Thus, apart from the fact that size effects are most likely interface related phenomena, careful analysis of literature data does not enable emergence of a consensual interpretation regarding the nature of the mechanism brought into play, even though in practice, one cannot rule out that different factors may indeed more or less influence the properties of ferroelectric thin film capacitors. In this paper, in order to discriminate which of the mechanisms mentioned above is the most suitable, we investigated PZT thin film capacitors with different thicknesses and electrode configuration. Careful examination of dielectric and ferroelectric properties enables to establish that variations in  $\epsilon_r$ ,  $E_c$ , and  $P_r$  values may basically be attributed to depolarization field inherent to interface chemistry, and particularly, to the interface located at the upper surface.

## II. EXPERIMENTAL

Platinum and lanthanum nickelate  $\text{LaNiO}_3$  (LNO) conducting oxide films were grown by rf magnetron sputtering. They were used either as bottom or top electrodes to inves-

<sup>a)</sup>Electronic mail: rachid.bouregba@ensicaen.fr.

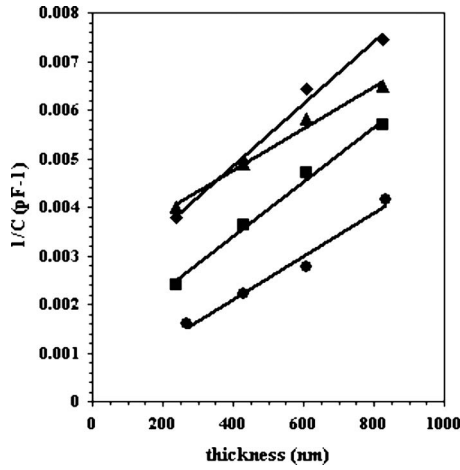


FIG. 1. Plot of the inverse of measured capacitance vs thickness with different electrode configurations: Pt/PZT/Pt/TiO<sub>x</sub>/SiO<sub>2</sub>/Si (diamonds), LNO/PZT/Pt/TiO<sub>x</sub>/SiO<sub>2</sub>/Si (squares), Pt/PZT/LNO/SiO<sub>2</sub>/Si (triangles), and LNO/PZT/LNO/SiO<sub>2</sub>/Si (circles). The frequency and the amplitude of the rf signal were 10 kHz and 0.1 V rms, respectively. VDC was 0 V.

tigate their effect on the dielectric and ferroelectric properties of Pb(Zr<sub>0.54</sub>Ti<sub>0.46</sub>)O<sub>3</sub> thin films with thicknesses ranging from 200 to 800 nm. To this end, four kinds of structures were processed on silicon substrate for comparison: Pt/PZT/Pt/TiO<sub>x</sub>/SiO<sub>2</sub>/Si, LNO/PZT/Pt/TiO<sub>x</sub>/SiO<sub>2</sub>/Si, Pt/PZT/LNO/SiO<sub>2</sub>/Si, and LNO/PZT/LNO/SiO<sub>2</sub>/Si. The PZT films were preferentially oriented along the (100) axis on LNO/Si and along (110) one on Pt/Si. More details regarding the conditions of preparation and structural characterization of these samples may be found elsewhere.<sup>23</sup>

Figure 1 displays the variation of the inverse of measured capacitance versus thickness, for each set of PZT capacitors. Linear change is obtained in agreement with the serial capacitance model which assumes regions with depressed dielectric properties in close vicinity of electrode-ferroelectric interfaces.<sup>5,10</sup> According to this model, the origin ordinate of the curve gives the interface capacitance ( $C_i$ ), whereas the slope informs about the bulk value of the dielectric constant ( $\epsilon_f$ ). The results are summarized in Table I and call for some remarks. The capacitors grown on the same bottom electrode show similar  $\epsilon_f$  whatever the nature of top electrode, what was expected since this quantity is determined by the crystallographic orientation of the film. PZT films on LNO/SiO<sub>2</sub>/Si exhibit larger  $\epsilon_f$  as compared to PZT films on Pt/TiO<sub>x</sub>/SiO<sub>2</sub>/Si. This difference is ascribed to different grain sizes achieved on both kinds of substrates. In this case, PZT films with LNO bottom electrode presented smaller grain size, as observed by scanning electronic microscopy. Second, as may be seen in Fig. 1, substitution of Pt by LNO as top electrode systematically leads to a significant improvement of the measured capacitance, thus of the dielec-

tric constant  $\epsilon_f$ . The strong contribution of the top Pt electrode in deterioration of the dielectric properties is materialized by achievement of smaller  $C_i$  values. The best structure in terms of measured capacitance is the one with LNO at both electrodes, which concomitantly presents the larger, but still finite,  $C_i$  value. Hence, on the basis of this model, we infer that (1) for a given thickness due to the voltage drop across the interface capacitance, the structures with top Pt electrode should involve the strongest external electric field to achieve saturation of the ferroelectric hysteresis loops. Hence greater elongation of the loops along electric field axis should be visible compared to structures with top LNO electrode. (2) As a corollary, the capacitors with top Pt electrode should require increasingly high maximum electric fields ( $E_{\max}$ ) with reduced thickness. (3) Elongation of the loops should be much less marked, but still observable, on the structures with LNO as top electrode. Figure 2 displays hysteresis loops measured on the four kinds of structures and Fig. 3 shows the effect of the nature of the structure for a given thickness. Some of the studied samples exhibit low leakage currents as attested by their open shaped hysteresis loops. However for convenience and simplicity of our analysis, their effects were neglected. The predictions above are verified, thereby corroborating the probable presence of passive layers with low permittivity at the interfaces. It must also be mentioned that elongation of the ferroelectric loops is conform to previous results of simulations that included non-switching interface dielectric layers.<sup>21,24,25</sup> However, two other noticeable facts may be picked up in Fig. 2: (1) Whatever the nature of the bottom electrode,  $E_c$  shows thickness dependence, i.e., increasingly large values with reduced thickness  $d$ , only when platinum is used as upper electrode, whereas no more variation of this quantity is observable when the latter is replaced by LNO. (2) Conversely, the remnant polarization  $P_r$  is almost independent of  $d$  when Pt is used as top electrode, whereas  $P_r$  starts to decrease below a certain thickness so long as LNO is used in its stead. These two observations, seemingly contradictory, raise the question of their connection with the existence of passive interface layers set forth above, or else, whether another mechanism must be invoked. Section III aims at clarifying this based on literature data.

### III. DISCUSSION

In a recent article, degradation in  $E_c$  values was accurately simulated on conditions to include nonferroelectric but charged layers at electrode-ferroelectric interfaces.<sup>26</sup> This necessity met the original proposition by other authors.<sup>20,22</sup> Interface charge gives rise to a built-in potential  $V_{bi}$  that can be estimated by plotting  $E_c$  versus  $1/d$ , according to the model detailed in Ref. 26. Figure 4 shows such plots for

TABLE I. Summary of the values extracted from the plot of  $1/C=f(d)$ . Area of the ferroelectric capacitors was  $1.8 \times 10^{-4}$  cm<sup>2</sup>.

	Pt/PZT/Pt/TiO <sub>x</sub> /SiO <sub>2</sub> /Si	LNO/PZT/Pt/TiO <sub>x</sub> /SiO <sub>2</sub> /Si	Pt/PZT/LNO/SiO <sub>2</sub> /Si	LNO/PZT/LNO/SiO <sub>2</sub> /Si
$\epsilon_f$	1070	1070	1600	1600
$C_i$ (nF)	0.435	0.91	0.33	3.33

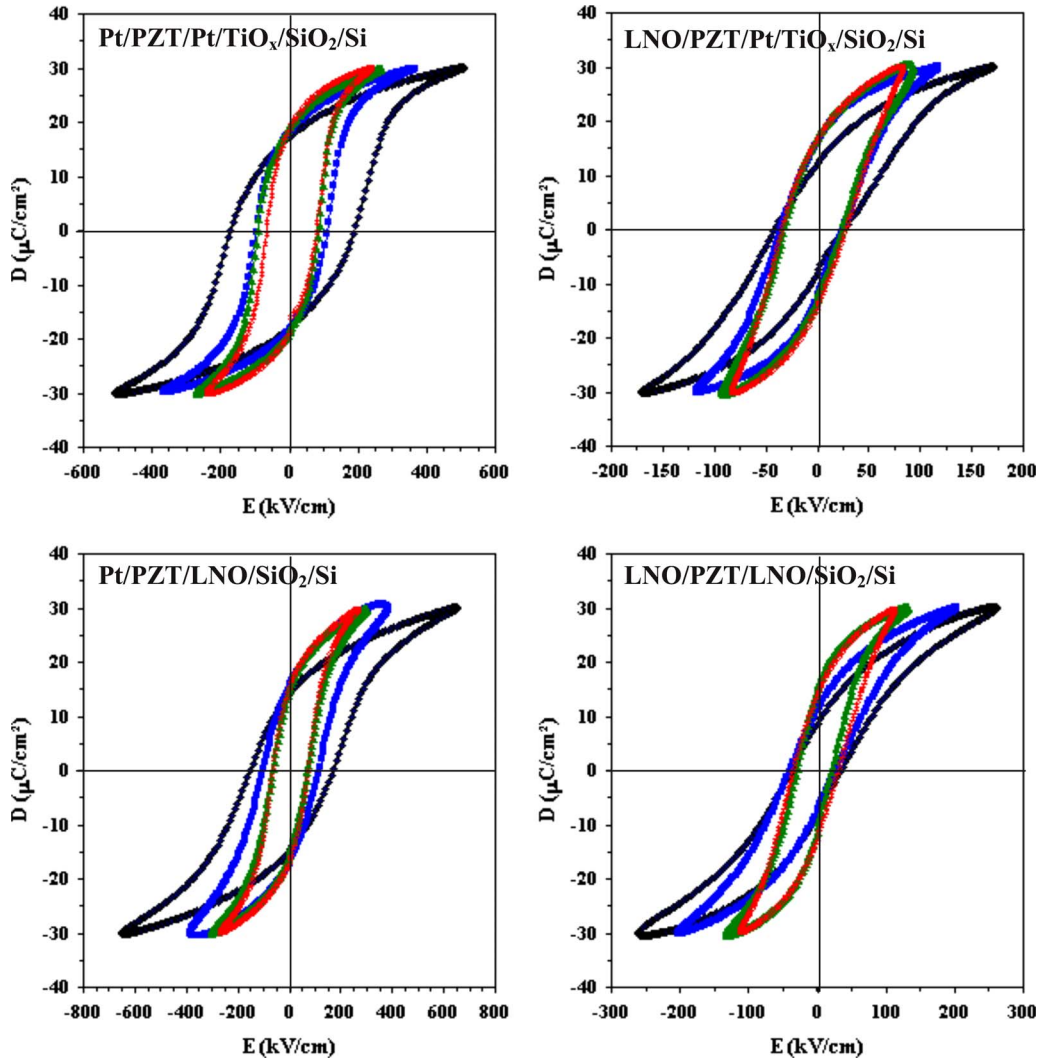


FIG. 2. (Color online) Hysteresis loops of the PZT capacitors with different electrode configurations and different thicknesses. Elongation of the loops is clearly visible as the thickness is reduced: black diamonds, blue squares, green triangles, red crosses for 240, 430, 610, and 830 nm, respectively. Note that for clarity of the plots,  $E$ -axes with different scales were used. Amplitude of the applied voltage was systematically adjusted in order to bring all the structures in the same condition of polarization, as determined by achievement of a same maximum electric displacement. The frequency measurement was 100 Hz.

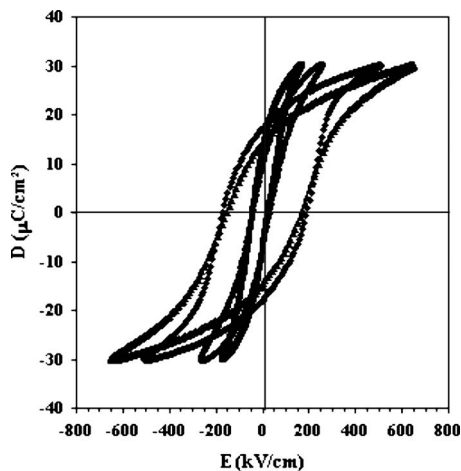


FIG. 3. Comparison of hysteresis loops measured on the four kinds of structures for a given thickness (240 nm): Pt/PZT/Pt/TiO<sub>x</sub>/SiO<sub>2</sub>/Si (diamonds), LNO/PZT/Pt/TiO<sub>x</sub>/SiO<sub>2</sub>/Si (squares), Pt/PZT/LNO/SiO<sub>2</sub>/Si (triangles), and LNO/PZT/LNO/SiO<sub>2</sub>/Si (circles).

Pt/PZT/LNO/SiO<sub>2</sub>/Si and LNO/PZT/LNO/SiO<sub>2</sub>/Si structures. Straight lines are obtained, the slope of which gives  $V_{bi}$ .<sup>26</sup> We found for these two structures:  $V_{bi}$  3.3 and 0.18 V, respectively. Very similar results were obtained for the two other structures grown on Pt/TiO<sub>x</sub>/SiO<sub>2</sub>/Si. Accordingly, it is likely that the PZT capacitors with top Pt electrode exhibit charged layer with strongly depressed dielectric properties at the upper interface. Substitution of Pt by LNO at this interface improves the dielectric properties of the surface layer and almost cancels the charge. The nature of the bottom electrode seems not to play a key role, apart from determining the crystallographic orientation. It must be emphasized that passive layers certainly enable to explain increase in  $E_{max}$ , i.e., elongation of the hysteresis loops when  $d$  is reduced, but is inappropriate to interpret the thickness dependence of  $E_c$  unless static potential resulting from interface charge is considered.<sup>20–22,26</sup>

The JKD theory<sup>3,15</sup> mentioned above, which predicts a  $d^{-2/3}$  scaling law for  $E_c$ , has been matter of debate. It has indeed been suggested to be irrelevant to the thickness dependence of  $E_c$ .<sup>27</sup> Arguments advanced were that the JKD

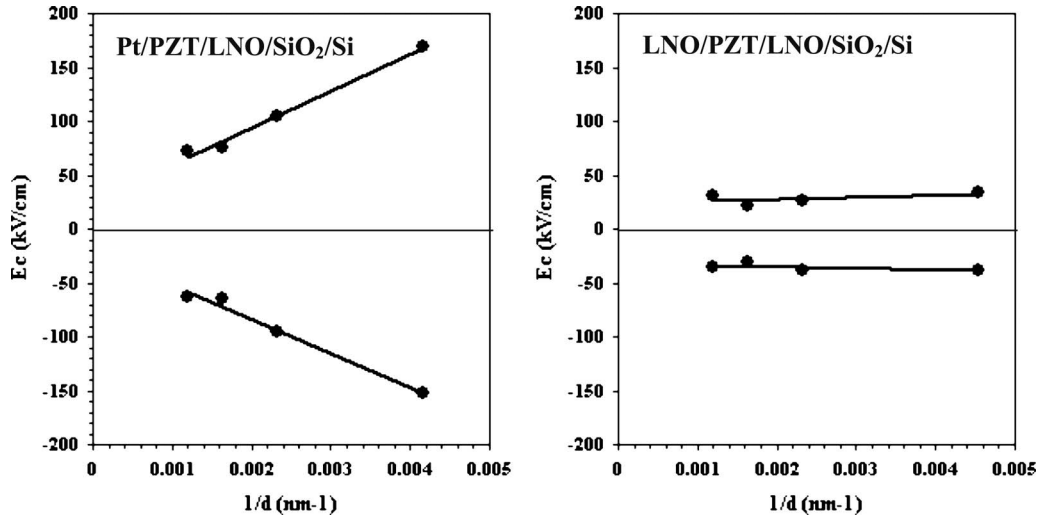


FIG. 4. Plot of coercive field  $E_c$  vs  $1/d$  according to the model detailed in Ref. 26, for Pt/PZT/LNO/Si and LNO/PZT/LNO/Si structures. The slope of the curve enables determination of the interface built-in potential  $V_{bi}$ . The higher the slope, the larger  $V_{bi}$ .

scaling law was derived by considering lattice with no defects,<sup>27</sup> and by assuming no internal electric field in the ferroelectric capacitor.<sup>28</sup> Our experimental results above seem to justify these criticisms as the thickness dependence of  $E_c$  observed on the structures with top Pt electrode, resulted most likely from presence of structural defects at the upper interface. Conversely the structures with LNO as top electrode, which displayed no change in  $E_c$  values, are likely to present a much less density of defects, in agreement with the reduced interface potential barrier determined above. This is consistent with the fact that LNO and PZT are of the same chemical nature with close lattice parameters. Moreover, it must be mentioned that ferroelectric capacitors exhibiting size dependence of  $E_c$  have been demonstrated to be also particularly prone to fatigue phenomenon.<sup>29,30</sup> Now, fatigue which was suspected to arise from presence of defects at interfaces,<sup>29-31</sup> is typically encountered on structures with at least one metallic electrode, whereas it is absent when oxide conducting electrodes are used.<sup>1,29,32</sup> Hence, size dependence of  $E_c$  requires extrinsic effects to be assumed, unlike as suggested by the JKD theory. Recently, inhomogeneous nucleation including nonzero depolarization field across the film due to finite screening length in the metal electrodes has been proposed as an alternative model to describe size dependence of  $E_c$  in ultrathin ferroelectric capacitors.<sup>28,33</sup> However according to this model, the ferroelectric capacitors with top LNO electrode should exhibit a stronger depolarization field, hence a more marked size dependence of  $E_c$ , as compared to those with top Pt electrode because oxide electrodes present larger field penetration due to lower carrier density. Now actually this is not the case. Moreover, if finite screening length in the electrodes was effectively the main cause, then one should obtain almost similar size dependence of  $E_c$  for Pt/PZT/LNO/SiO<sub>2</sub>/Si and LNO/PZT/Pt/TiO<sub>x</sub>/SiO<sub>2</sub>/Si structures. Indeed, the conditions of preparation of Pt or LNO layers, although being slightly different depending on whether one considers the top or the bottom electrode,<sup>23</sup> are not expected to yield significantly different carrier densities, hence different screening

lengths, to justify observation of size dependence of  $E_c$  in one case and not in the other. Totally different behaviors were yet observed on these two structures (see Figs. 2 and 3). Therefore, one can reasonably rule out surface nucleation and finite screening length in the electrodes for the interpretation of the thickness dependence of  $E_c$  in our ferroelectric structures.

In so far the idea of depolarization field ( $E_{dep}$ ) must not be rejected. Originally, incomplete compensation of surface charge by free charges in the electrodes, therefore the resulting depolarizing field, has been invoked to be responsible for the decrease in polarization with reduced thickness, but also to analyze the problem of stability and retention of polarization in ferroelectric films.<sup>16-18</sup> The crucial role of such a field in the suppression of ferroelectricity was confirmed by first-principles calculations<sup>19</sup> and shown to play a prominent role through direct measurements of polarization in PZT and BTO ultrathin film capacitors with SrRuO<sub>3</sub> electrodes.<sup>12-14</sup> However, the arguments we developed above suggest that if a depolarization field is likely to occur in our films, the latter probably arose from region with depressed dielectric properties at the upper surface of the film, rather than from finite screening length in the top electrode. The idea of existence of space charge layer at the surface of ferroelectric films is not new and was first suggested by Känzig.<sup>34</sup>

From a strict formalism view point, analogous relations may be obtained for  $E_{dep}$  in both cases. Expressions of the surface charge density on the capacitor plates ( $D$ ) and the electric field applied to the bulk ferroelectric layer ( $E_f$ ) have been established within the framework of the model of non-ferroelectric charged layers at electrode-ferroelectric interfaces [see relations (1) and (2) in Ref. 26]. From these two expressions and considering the short circuit situation because we focus on the remnant value of  $D$  ( $D_r$ ), one obtains

$$D_r = \left[ -\frac{\epsilon_o \epsilon_f}{d} V_{bi} + P_f \left( 1 - \frac{d_i}{d} \right) \right] \frac{1}{\alpha} \quad (1)$$

and

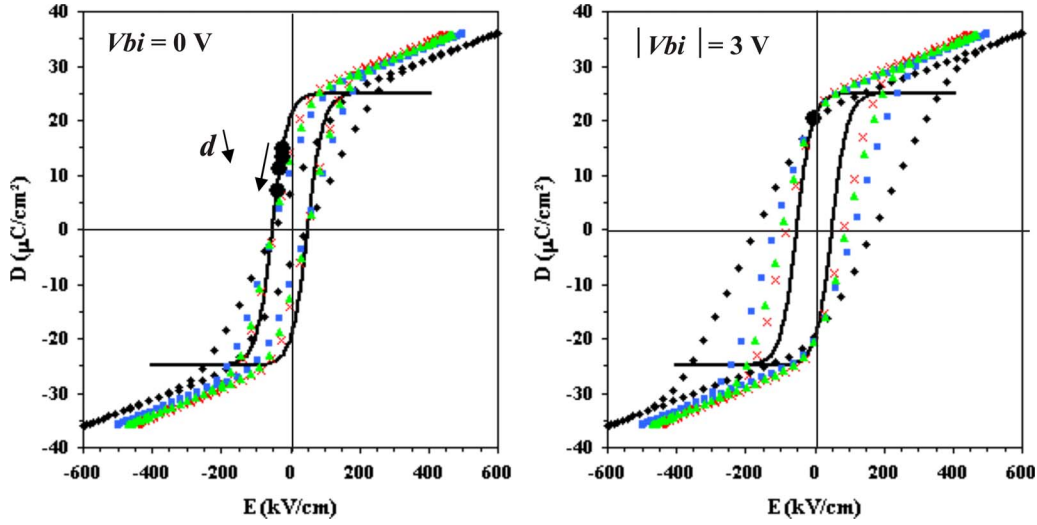


FIG. 5. (Color online) Set of  $D$ - $E$  hysteresis loops simulated from the model presented in Ref. 26. Black diamonds, blue squares, green triangles, red crosses for 200, 400, 600, and 800 nm thick films, respectively. In solid line is the inner  $P_f$ - $E_f$  loop, i.e., the polarization due to the switching domains in the bulk ferroelectric layer from which were computed all the external  $D$ - $E$  loops. The parameters used were the same as in Ref. 26 except those regarding the interface, chosen in such way that  $|V_{bi}|=3$  and 0 V. The large full circles on the inner loop materialize the values of  $P_f$  and  $E_f$  picked up at the time when  $D$  reaches its positive remnant value for each thickness, i.e., when  $V_{appl}=0$ . For  $V_{bi}=0$ , the bulk ferroelectric layer deviates from its remnant state as  $d$  decreases (the arrow indicates the direction of decreasing thickness). For  $|V_{bi}|=3$  V, the polarization operating point was almost stationary due to screening of the depolarization field by interface space charge.

$$E_{dep} = - \left[ V_{bi} + \frac{P_f d_i}{\epsilon_o \epsilon_i} \right] \frac{1}{d\alpha}, \quad (2)$$

with

$$\alpha = 1 - \frac{d_i}{d} + \frac{\epsilon_f d_i}{d \epsilon_i}.$$

$\epsilon_o$  is the permittivity of free space,  $P_f$  is the polarization in the bulk ferroelectric layer,  $d_i$  the total thickness, and  $\epsilon_i$  is the permittivity of the interface layers. The other parameters have already been defined. In the special situation where  $d_i \ll d$ ,  $E_{dep}$  becomes

$$E_{dep} = - \left[ \frac{V_{bi}}{\left( d + \frac{\epsilon_f d_i}{\epsilon_i} \right)} + \frac{P_f}{\epsilon_o \epsilon_f} \left( \frac{\frac{\epsilon_f}{d}}{\frac{\epsilon_i}{d_i} + \frac{\epsilon_f}{d}} \right) \right]. \quad (3)$$

Expression (3) above is similar to expression (16) of  $E_{dep}$  found in Ref. 17, except for the presence of the first term including  $V_{bi}$ . So the previous treatments of loss of polarization that were based on depolarization field from electrodes are presumed to still apply if  $E_{dep}$  arises, instead, from a nonferroelectric layer at the upper surface of the PZT film. This was expected because in both cases and in the short circuit situation,  $E_{dep}$  just results from existence of a nonzero voltage across the bulk ferroelectric layer that is equal and opposite to the voltage drop across interface regions where the polarization is assumed to vanish.  $E_{dep}$  is suppressed when these interface regions no more exist, i.e., when  $C_i$  is infinite and  $V_{bi}$  is null.

The presence of  $V_{bi}$  is very crucial in understanding the behavior of the remnant values of  $D$  observed in Fig. 2. It has been established that correct simulation of the thickness dependence of  $E_c$  requires the sign of  $V_{bi}$  to be changed

according to the time derivative of the applied voltage ( $V_{appl}$ ) (Ref. 26). For instance when  $\delta V_{appl}/\delta t$  is negative, i.e., when the electric displacement changes from its maximum positive value ( $+D_m$ ) to its maximum negative one ( $-D_m$ ),  $V_{bi}$  must be negative. In that case expression (2) above shows that interface charge tends to oppose the depoling effect of the polarization in the bulk ferroelectric layer, i.e., to lower  $E_{dep}$  since then  $P_f$  is positive. As a result, the remnant value of  $D$  considered here, i.e.,  $D_{r+}$ , should exhibit a thickness dependence more or less attenuated, according to the magnitude of  $V_{bi}$  [see relation (1)]. It should even be possible to achieve increasing  $D_{r+}$  with reduced thickness if  $V_{bi}$  is high enough. On the contrary, structures in which  $V_{bi}$  is almost negligible should experience stronger depolarizing field associated with a marked thickness dependence of  $D_{r+}$ . It is understood that the same conclusions may be drawn when considering  $D_{r-}$ , which belongs to that part of the loop where  $D$  changes from  $-D_m$  to  $+D_m$  since then  $V_{bi} > 0$  but  $P_f < 0$ .<sup>26</sup> In the light of this analysis, the apparent contradiction underlined above when analyzing the hysteresis measurements can now be clarified. It is the presence of high density of interface charged defects in the structures with Pt as top electrode which caused  $E_c$  to increase when downscaling, but at the same time made  $D_r$  almost constant because the large value of  $V_{bi}$  screened  $E_{dep}$ . On the contrary the better interface achieved with LNO, with probably much less density of charged defects, made  $E_c$  much less sensible to thickness variations. In that case however, unscreened depoling field strongly influenced  $D_r$  below a certain thickness because this interface still presented depressed dielectric properties, materialized by the high but finite value of  $C_i$ . Figure 5 shows the results of simulations performed from the model developed in Ref. 26, which clearly support the analysis above (the meaning of the large full circles is addressed further).

It must be noted that the polarization term  $P_f$  in relations

(1) and (2) cannot be the remnant value ( $P_{fr}$ ) even though we treated the short circuit situation where  $V_{\text{appl}}=0$  and  $D=D_r$ . In other words, distinction must be made between  $D_r$  measured on the plates of the ferroelectric capacitor, and  $P_{fr}$  due to the switching domains. Indeed if  $P_f=P_{fr}$ , then the electric field in the bulk ferroelectric layer  $E_f$ , hence  $E_{\text{dep}}$ , has to be null due to the relationship between  $P_f$  and  $E_f$  imposed by the inner polarization loop. We infer from relation (2) that existence of  $E_{\text{dep}}$  leads the bulk ferroelectric layer to deviate from the remnant state *even though the ferroelectric capacitor get it*.

Moreover relation (1) suggests that the decrease in  $D_r$  with thickness occurs according to  $[(d-d_i)/(d-d_i+K)]$  scaling law, where  $K$  is a constant (for convenience and simplicity of analysis we consider the case where  $V_{\text{bi}}=0$ ). This law is only valid if  $P_f$  is constant, but actually  $P_f$  decreases likewise with downscaling, which contributes to exacerbate the decrease in  $D_r$  for thicknesses small enough. Indeed, from relation (2) we see that any reduction in the thickness tends to increase the depolarizing field strength. This drives the bulk ferroelectric layer to deviate further from the remnant state and therefore  $P_f$  is likely to decrease. For each thickness the system reaches a new equilibrium state which may be found by solving Eq. (2) and the inner  $P_f$ - $E_f$  polarization loop. This is illustrated on Fig. 5. Simulations were performed by utilizing hyperbolic tangent function for the description of  $P_f$ - $E_f$  polarization loop.<sup>24,26</sup> The change in the shape of the external loops with the thickness is in good agreement with that of the experimental ones (Fig. 2) and with discussion above. The presence of interface charge hinders the occurrence of depolarizing field, thereby limiting the decrease in  $P_f$  and  $D_r$ . Finally the apparent accelerated loss of *external* polarization that may be observed with downscaling must not be seen as the consequence of degradation of the bulk ferroelectric properties, but as the result of shifting of the operating point along the *inner* polarization loop, the intrinsic properties of which may be considered invariant with downscaling, within the range of thicknesses investigated here.

This last assertion follows the previous experimental works by Ducharme *et al.*,<sup>8</sup> Bune *et al.*,<sup>35</sup> and Fong *et al.*<sup>36</sup> who concluded that stable intrinsic ferroelectricity may be observed on ferroelectric ultrathin films until thickness is down to only few monolayers. It has been proposed that stabilization of ferroelectricity in thin films may be due to a thickness dependent built-in internal field arising from film-substrate mismatch effect and piezoelectricity that has to exist in the vicinity of the films surface.<sup>37,38</sup> Such built-in field is likely to play an essential role in ultrathin films, particularly in those showing epitaxial growth because the mechanical strains are most important in that case. However our investigation does not concern the same scale of thickness since the latter was far beyond 100 nm. We believe indeed that in our films the effect of such built-in field, even if it existed, may be neglected and this is all the more warranted as our films were not epitaxial. The intrinsic properties we discussed in our model above are relating to those of the bulk material, obtained after removing extrinsic effects due to the interface defects. Therefore it is clear that the model pre-

sented in this article is not immediately applicable for the analysis of ultrathin films and has, before, to be improved by including the effect of film-substrate mismatch, as described in Refs. 37 and 38.

#### IV. SUMMARY AND CONCLUSIONS

In this work, degradation of dielectric and ferroelectric properties were observed on PZT capacitors when their thickness is reduced. The deterioration was more or less marked according to the nature of the electrode used at the top surface. In agreement with many previous works, the decrease in  $\epsilon_r$  was explained by existence of region with depressed properties at the upper surface, particularly when metallic electrode was used. This interface region appeared to be much less imperfect when conducting oxide electrode was employed. On the other hand we showed that an increase in  $E_c$  and a decrease in  $P_r$  were not concomitant, i.e., degradation of one value did not necessarily come with the degradation of the other. In fact, existence of a depolarization field enabled to explain the loss of polarization, as commonly accepted in literature. However, in this work it was shown that this field probably arose from interface chemistry, unlike suggested in previous works where finite screening length in electrodes was invoked. On the other hand, such field alone was not sufficient to interpret the observed variation of coercive field and static potential associated with interface charged defects must be considered. The latter, suspected to be present with high density when using Pt electrode, contributed to screen the depolarizing field and thus to strongly attenuate the decrease in  $P_r$  values with downscaling, unlike what was observed when oxide electrode was used. We conclude that the main features of size effects observed on our structures were mainly governed by extrinsic effects, specifically by electrostatics in relation with interface chemistry rather than finite screening length in the electrodes. Detrimental effects of downscaling can be significantly limited by using oxide conducting electrode at the upper surface, whereas use of metallic electrode on substrate side is not problematic. Fatigue measurements are in progress to check whether these conclusions may be generalized or not to this source of failure.

<sup>1</sup>J. F. Scott, *Ferroelectric Memories* (Springer, New York, 2000).

<sup>2</sup>W. J. Merz, *J. Appl. Phys.* **27**, 938 (1956).

<sup>3</sup>H. F. Kay and J. W. Dunn, *Philos. Mag.* **7**, 2027 (1962).

<sup>4</sup>Y. Sakashita, H. Segawa, K. Tominaga, and M. Okada, *J. Appl. Phys.* **73**, 7857 (1993).

<sup>5</sup>P. K. Larsen, G. J. M. Dormans, D. J. Taylor, and P. J. van Veldhoven, *J. Appl. Phys.* **76**, 2405 (1994).

<sup>6</sup>A. K. Tagantsev, C. Z. Pawlaczyk, K. Brooks, and N. Setter, *Integr. Ferroelectr.* **4**, 1 (1994).

<sup>7</sup>S. B. Ren, C. J. Lu, J. S. Liu, H. M. Shen, and Y. N. Wang, *Phys. Rev. B* **54**, R14337 (1996).

<sup>8</sup>S. Ducharme, V. M. Fridkin, A. V. Bune, S. P. Palto, L. M. Blinov, N. N. Petukhova, and S. G. Yudin, *Phys. Rev. Lett.* **84**, 175 (2000).

<sup>9</sup>N. A. Pertsev, J. Rodriguez Contreras, V. G. Kukhar, B. Hermanns, H. Kohlstedt, and R. Waser, *Appl. Phys. Lett.* **83**, 3356 (2003).

<sup>10</sup>T. Hase, T. Sakuma, Y. Miyasaka, K. Hirata, and N. Hosokawa, *Jpn. J. Appl. Phys., Part 1* **32**, 4061 (1993).

<sup>11</sup>J. J. Lee, C. L. Thio, and S. B. Desu, *J. Appl. Phys.* **78**, 5073 (1995).

<sup>12</sup>V. Nagarajan, S. Prasertchoung, T. Zhao, H. Zheng, J. Ouyang, R. Ramesh, W. Tian, X. Q. Pan, D. M. Kim, C. B. Eom, H. Kohlstedt, and R. Waser, *Appl. Phys. Lett.* **84**, 5225 (2004).



- <sup>13</sup>Y. S. Kim, D. H. Kim, Y. J. Chang, T. W. Noh, J. H. Kong, K. Char, Y. D. Park, S. D. Bu, J.-G. Yoon, and J.-S. Chung, *Appl. Phys. Lett.* **86**, 102907 (2005).
- <sup>14</sup>Y. S. Kim, J. Y. Jo, D. J. Kim, Y. J. Chang, J. H. Lee, T. W. Noh, T. K. Song, J.-G. Yoon, J.-S. Chung, S. I. Baik, Y.-W. Kim, and C. U. Jung, *Appl. Phys. Lett.* **88**, 072909 (2006).
- <sup>15</sup>V. Janovec, *Czech. J. Phys., Sect. A* **8**, 3 (1958).
- <sup>16</sup>I. P. Batra and B. D. Silverman, *Solid State Commun.* **11**, 291 (1972).
- <sup>17</sup>R. R. Mehta, B. D. Silverman, and J. T. Jacobs, *J. Appl. Phys.* **44**, 3379 (1973).
- <sup>18</sup>P. Würfel and I. P. Batra, *Ferroelectrics* **12**, 55 (1976).
- <sup>19</sup>J. Junquera and P. Ghosez, *Nature (London)* **422**, 506 (2003).
- <sup>20</sup>A. K. Tagantsev and I. A. Stolichnov, *Appl. Phys. Lett.* **74**, 1326 (1999).
- <sup>21</sup>A. K. Tagantsev, M. Landivar, E. Colla, and N. Setter, *J. Appl. Phys.* **78**, 2623 (1995).
- <sup>22</sup>J. F. M. Cillessen, M. W. J. Prins, and R. M. Wolf, *J. Appl. Phys.* **81**, 2777 (1997).
- <sup>23</sup>N. Sama, R. Herdier, D. Jenkins, C. Soyer, D. Remiens, M. Detalle, and R. Bouregba, *J. Cryst. Growth* **310**, 3299 (2008).
- <sup>24</sup>S. L. Miller, R. D. Nasby, J. R. Schwank, M. S. Rodgers, and P. V. Dressendorfer, *J. Appl. Phys.* **68**, 6463 (1990).
- <sup>25</sup>C. J. Brennan, *Ferroelectrics* **132**, 245 (1992).
- <sup>26</sup>R. Bouregba, G. Le Rhun, G. Poullain, and G. Leclerc, *J. Appl. Phys.* **99**, 034102 (2006).
- <sup>27</sup>A. K. Tagantsev, *Integr. Ferroelectr.* **16**, 237 (1997).
- <sup>28</sup>M. Dawber, P. Chandra, P. B. Littlewood, and J. F. Scott, *J. Phys.: Condens. Matter* **15**, L393 (2003).
- <sup>29</sup>H. Z. Jin and J. Zhu, *J. Appl. Phys.* **92**, 4594 (2002).
- <sup>30</sup>I. Stolichnov, A. Tagantsev, E. Colla, S. Gentil, S. Hiboux, J. Baborowski, P. Muralt, and N. Setter, *J. Appl. Phys.* **88**, 2154 (2000).
- <sup>31</sup>G. Le Rhun, G. Poullain, and R. Bouregba, *J. Appl. Phys.* **96**, 3876 (2004).
- <sup>32</sup>R. Ramesh, W. K. Chan, B. Wilkens, H. Gilchrist, T. Sands, J. M. Tarascon, V. G. Keramidas, D. K. Fork, J. Lee, and A. Safari, *Appl. Phys. Lett.* **61**, 1537 (1992).
- <sup>33</sup>arXiv:cond-mat/0206014.
- <sup>34</sup>W. Känzig, *Phys. Rev.* **98**, 549 (1955).
- <sup>35</sup>A. V. Bune, V. M. Fridkin, S. Ducharme, L. M. Blinov, S. P. Palto, A. V. Sorokin, S. G. Yudin, and A. Zlatkin, *Nature (London)* **391**, 874 (1998).
- <sup>36</sup>D. D. Fong, G. B. Stephenson, S. K. Streiffer, J. A. Eastman, O. Auciello, P. H. Fuoss, and C. Thompson, *Science* **304**, 1650 (2004).
- <sup>37</sup>M. D. Glinchuk and A. N. Morozovska, *J. Phys.: Condens. Matter* **16**, 3517 (2004).
- <sup>38</sup>M. D. Glinchuk, E. A. Eliseev, and A. N. Morozovska, *Ferroelectrics* **354**, 86 (2007).